



This is a repository copy of *Integrating planar polarity and tissue mechanics in computational models of epithelial morphogenesis*.

White Rose Research Online URL for this paper:
<http://eprints.whiterose.ac.uk/122836/>

Version: Accepted Version

Article:

Fisher, K.H., Strutt, D. and Fletcher, A.G. orcid.org/0000-0003-0525-4336 (2017) Integrating planar polarity and tissue mechanics in computational models of epithelial morphogenesis. *Current Opinion in Systems Biology*, 5. pp. 41-49. ISSN 2452-3100

<https://doi.org/10.1016/j.coisb.2017.07.009>

Article available under the terms of the CC-BY-NC-ND licence
(<https://creativecommons.org/licenses/by-nc-nd/4.0/>).

Reuse

This article is distributed under the terms of the Creative Commons Attribution-NonCommercial-NoDerivs (CC BY-NC-ND) licence. This licence only allows you to download this work and share it with others as long as you credit the authors, but you can't change the article in any way or use it commercially. More information and the full terms of the licence here: <https://creativecommons.org/licenses/>

Takedown

If you consider content in White Rose Research Online to be in breach of UK law, please notify us by emailing eprints@whiterose.ac.uk including the URL of the record and the reason for the withdrawal request.



eprints@whiterose.ac.uk
<https://eprints.whiterose.ac.uk/>

1 **Integrating planar polarity and tissue mechanics in computational models of**
2 **epithelial morphogenesis**

3

4 Katherine H. Fisher^{1,2}

5 David Strutt^{1,2}

6 Alexander G. Fletcher^{1,3,*}

7

8 1 Bateson Centre, University of Sheffield, Firth Court, Western Bank, Sheffield, S10
9 2TN

10 2 Department of Biomedical Science, University of Sheffield, Firth Court, Western
11 Bank, Sheffield, S10 2TN

12 3 School of Mathematics and Statistics, University of Sheffield, Hicks Building,
13 Hounsfield Road, Sheffield, S3 7RH

14

15 * Corresponding author: a.g.fletcher@sheffield.ac.uk

16

17

18 **Abstract**

19

20 Cells in many epithelial tissues are polarised orthogonally to their apicobasal axis.
21 Such planar polarity ensures that tissue shape and structure are properly organised.
22 Disruption of planar polarity can result in developmental defects such as failed neural
23 tube closure and cleft palate. Recent advances in molecular and live-imaging
24 techniques have implicated both secreted morphogens and mechanical forces as
25 orienting cues for planar polarisation. Components of planar polarity pathways act
26 upstream of cytoskeletal effectors, which can alter cell mechanics in a polarised
27 manner. The study of cell polarisation thus provides a system for dissecting the
28 interplay between chemical and mechanical signals in development. Here, we
29 discuss how different computational models have contributed to our understanding of
30 the mechanisms underlying planar polarity in animal tissues, focusing on recent
31 efforts to integrate cell signalling and tissue mechanics. We conclude by discussing
32 ways in which computational models could be improved to further our understanding
33 of how planar polarity and tissue mechanics are coordinated during development.

34 Introduction

35

36 A central problem in developmental biology is to understand how tissues form and
37 repair in a highly reproducible manner. Key signalling molecules are spatially
38 coordinated to provide positional information in developing tissues. While it has long
39 been known that cells can sense and interpret such chemical gradients during
40 pattern formation [1], mechanical forces are now recognised to also play a vital role
41 in shaping tissues [2,3]. Increasing evidence suggests that these chemical and
42 physical mechanisms are interconnected [4].

43

44 Morphogenesis is frequently driven by the dynamics of epithelial tissues, which line
45 the majority of organs in the body. As well as being characterised by polarity along
46 an apicobasal axis, epithelia often exhibit planar polarity orthogonally through the
47 plane of the tissue (**Fig. 1A**) [5]. While it is possible for individual cells to become
48 planar polarised, animal epithelial cells locally coordinate their polarity via
49 intercellular transmembrane complexes (**Fig. 1B**) [6,7] to robustly generate uniform
50 polarity across tissues, even when a global polarising signal is weak or noisy [8,9].

51

52 This coordinated polarity can be readily visualised by the formation of oriented
53 external structures such as hairs or bristles (**Fig. 1B, C**). It is also vital for
54 fundamental functional roles that require cell coordination, such as oriented division
55 (**Fig. 1D**) and convergent extension (**Fig. 1E**), thus disruption of these mechanisms
56 results in disease [10]. Research into planar polarity establishment focuses on how
57 long-range morphogen and mechanical gradients are interpreted at the cellular level
58 [11], how cells communicate to coordinate information from upstream cues [12], and
59 how downstream effectors alter cell behaviour and the forces underlying tissue
60 formation [13].

61

62 Given the complexity of these processes, computational modelling plays an
63 increasingly useful role in aiding our mechanistic understanding [14]. A key challenge
64 is to interface models that include descriptions of cell shape, mechanics, and
65 signalling on different scales. In this review, we consider the contribution of
66 computational modelling first to planar polarity establishment, then to downstream
67 mechanics, and the novel computational methods that study the interplay between
68 them. For brevity, we consider animal tissues only, focussing primarily on *Drosophila*
69 since the majority of planar polarity components have been extensively studied in
70 that system.

71 **Modelling planar polarity establishment**

72

73 Planar polarity can refer to any polarised protein or structure that breaks cellular
74 symmetry in the plane of the tissue, occurring via multiple independent pathways.

75 We begin by briefly summarising computational modelling of two key pathways: the
76 Frizzled (Fz)-dependent or 'core' pathway, and the Fat (Ft)-Dachsous (Ds) pathway.

77 We then describe the conserved anteroposterior (AP) patterning system active in the
78 *Drosophila* embryonic epidermis.

79

80 *Core pathway*

81

82 Components of the core pathway form asymmetrically localised molecular bridges
83 between cells. The transmembrane protein Flamingo (Fmi; Celsr in vertebrates) can
84 homodimerise via its extracellular domain across *intercellular* junctions. Fmi interacts
85 *intracellularly* with two other transmembrane proteins, Fz and Van Gogh (Vang),
86 which recruit several cytoplasmic factors (**Fig. 2A**). Since Fmi can homodimerise, it
87 exhibits axial asymmetry (enriched on both sides of cells), whereas all other factors
88 exhibit vectorial asymmetry (enriched on one side) (**Fig. 1A**). Fz and Vang appear to
89 be the key components for recruiting other factors to apical junctional domains [15]
90 and mediating cell communication of polarity [16,17], whereas the cytoplasmic
91 proteins are thought to be responsible for polarity establishment [18-20] by amplifying
92 initial asymmetries in Fmi, Fz and Vang through feedback interactions. The outcome
93 of this pathway dictates, for example, the orientation of hairs on the *Drosophila* wing
94 surface (**Fig. 1B, C**).

95

96 A variety of mathematical models have been proposed for the molecular wiring
97 underlying this amplification [21]. In these models, asymmetric complexes form at
98 cell junctions and feedback interactions occur between complexed proteins, such
99 that either 'like' complexes of the same orientation are stabilised, or 'unlike'
100 complexes of opposite orientation are destabilised, generating bistability (**Fig. 2B**).
101 These models vary in complexity and include those based on Turing pattern
102 formation mechanisms, using deterministic [22,23] or stochastic [24] reaction-
103 diffusion approaches, and others based on the Ising model of ferromagnetism, which
104 treat each cell as a 'dipole' that locally coordinates its angle with its neighbours [25].
105 Such models also vary in biological detail; from abstracted systems where two
106 species bind to form a complex at junctions [26,27] to those including more defined
107 molecular species. The latter necessitates many more kinetic parameters: for

108 example, the model by Amonlirdviman et al [22] contains nearly 40 rate constants,
109 diffusion coefficients and conserved concentrations whose values had to be
110 estimated.

111

112 Domineering non-autonomous phenotypes, where a clone of cells mutant for a
113 polarity protein influences the polarity of wild-type neighbours (**Fig. 2C**), have formed
114 the basis for validating core pathway models at the tissue scale. Whether considering
115 a one-dimensional row of two-sided cells [27], or a two-dimensional field of
116 hexagonal [22] or irregularly shaped cells [28], various models are able to
117 recapitulate these phenotypes. Importantly, modelling has bolstered our intuition on
118 how polarity may be established and highlighted critical conceptual factors necessary
119 for the system to work. For example, both the Amonlirdviman [22] and Le Garrec [24]
120 models can generate tissue-level planar polarity when provided with a transient,
121 rather than sustained, polarity cue; however, transient cues are not sufficient to
122 ensure robustness of the resulting cellular polarisation (**Fig. 2D**) [23]. A number of
123 biological candidates for a persistent global bias have been suggested, including the
124 directional trafficking of Fz complexes along microtubules [29,30].

125

126 *Ft-Ds pathway*

127

128 In contrast to the core pathway, there is strong evidence for a primary role of
129 morphogen gradients in orienting the Ft-Ds pathway. In developing tissues, upstream
130 morphogens specify opposing tissue gradients of Four-jointed (Fj), a Golgi-tethered
131 kinase and Ds, a cadherin [31]. Ft and Ds are single-pass transmembrane proteins
132 that can heterodimerise across intercellular cell junctions (**Fig. 3A**). They are both
133 phosphorylated by Fj, which alters their ability to bind to one another [32,33].
134 Interestingly, although similar domains are modified on each protein, phosphorylation
135 of Ft appears to improve its ability to bind to Ds, while phosphorylation of Ds is
136 inhibitory. Work in *Drosophila* shows that Ft and Ds become asymmetrically localised
137 within cells and that in turn recruits the atypical myosin Dachs to the distal side of
138 cells [33-35]. Polarisation of this pathway can regulate tissue growth via the Hippo
139 signalling pathway [36] and tissue shape by modulating tension at cell-cell junctions
140 and orienting cell divisions [34,37,38], as well as coupling to the core pathway via the
141 Pk isoform, Spiny-legs (Sple) [39].

142

143 While abstracted planar polarity models [8,26,27] could in principle be applied to the
144 Ft-Ds system, models tailored to specific molecular interactions are limited. A recent

145 phenomenological model examined the collective polarisation of the predominant
146 complex – phosphorylated Ft (Ft^P) binding unphosphorylated Ds (Ds^U) – between
147 cells in the *Drosophila* wing [40]. Either stabilising or destabilising feedback was
148 found to amplify shallow graded inputs, but a combination of both more readily
149 recapitulated experimental observations. By linking the strength of polarisation to a
150 downstream tissue growth parameter, predictions were made and tested about the
151 relationship between protein levels and overall tissue size.

152

153 Elsewhere, further molecular detail was included in a system of coupled ordinary
154 differential equations describing interactions, again forming the predominant complex
155 (Ft^P binding Ds^U), in a one-dimensional row of cells [41]. However, for the majority of
156 this study, the authors did not consider the orientation of those complexes at
157 individual junctions, but only the asymmetry of total complexes across each cell, thus
158 questions related to Ft and Ds polarity were not addressed. A more recent study
159 used the *Drosophila* larval wing disc (**Fig. 3B**) to quantify the Fj gradient and Ds
160 levels to initialise a one-dimensional reaction-diffusion model (**Fig. 3C**) [42]. Including
161 all possible complexes of phosphorylated and unphosphorylated forms of Ft and Ds
162 led to more uniform cellular polarity across the tissue (**Fig. 3D**). However, only
163 considering the most favoured complex, as in previous models, resulted in greater
164 variation in polarity and binding levels across the tissue. Coupled with experimental
165 evidence, this supports the hypothesis that Fj acts on both Ft and Ds *in vivo*, but with
166 opposing consequences, and illustrates the power of combining experimental and
167 theoretical approaches in the same work.

168

169 *AP patterning system*

170

171 In the *Drosophila* embryo, elongation of the body axis, known as germ-band
172 extension, is driven by polarised cell movements and appears to occur independently
173 of the core and Ft-Ds pathways [43]. Instead, evidence suggests that it is guided by
174 striped pair-rule gene expression [44,45], although some contribution is also afforded
175 to oriented cell divisions [46] and large-scale mechanical deformations [47]. The
176 complex upstream gene-regulatory network consists of maternally derived
177 morphogen gradients patterning gap gene expression, leading to stripes of pair-rule
178 gene expression [48]. While the gap gene network has been extensively studied
179 theoretically, uncovering shifting expression boundaries and the importance of
180 transient dynamics of gene regulation [49,50], modelling of striped pair-rule gene
181 expression and downstream processes remains limited.

182 **Modelling planar polarity pathway regulation of cell mechanics**

183

184 The importance of mechanics in epithelial morphogenesis is well established [51].
185 Furthermore, increasing evidence suggests that a common role of planar polarity
186 pathways is the spatial patterning of cell mechanics to affect consequent tissue-level
187 morphogenetic processes such as convergent extension. Studies in both *Drosophila*
188 and vertebrates reveal that downstream effectors include regulators of myosin II,
189 actin and cadherins [52,53], which in turn affect anisotropy of local forces within an
190 epithelial tissue (**Fig. 4A**). For example, the core planar polarity pathway has been
191 implicated in polarised modulation of cell adhesion through trafficking of the
192 adherens junction molecule E-cadherin. This appears to influence cell packing in the
193 *Drosophila* wing and cell intercalation in the trachea [54,55].

194

195 Nevertheless, models of polarity establishment typically assume that the dynamics of
196 protein localisation occurs on a much faster timescale than cell shape changes, and
197 thus consider a static cell packing geometry. To study dynamic cell shape changes
198 requires coupling of models of planar polarity with tissue mechanics. To this end a
199 variety of 'cell-based' models have been developed, which allow for the incorporation
200 of cell signalling and feedback [56]. These include vertex [57] and cellular Potts [58]
201 models, which approximate each cell's apical surface by a polygon whose vertices
202 move according to a force balance equation, or a set of pixels that change
203 stochastically to minimize an energy function, respectively (**Fig. 4B**). Each approach
204 has its strengths and limitations [59]. Here we discuss a number of example studies.

205

206 *Core pathway*

207

208 Inspired by evidence that the core planar polarity pathway can modulate cell
209 mechanics, Salbreux et al [60] applied a vertex model to the ordered packing of cells
210 in the zebrafish retina. Using a phenomenological differential equation model of
211 planar polarity protein dynamics, the authors assumed that protein localisation
212 modulates the 'surface tension' associated with cell-cell junctions and – through force
213 balance – cell and tissue geometry. Geometry then feeds back on the localisation of
214 planar polarity proteins. By comparing simulations under different hypotheses, the
215 authors deduced that an extrinsic force (intraocular pressure) and progressive cell
216 growth and division were required for the observed packing behaviour. Importantly,
217 the authors tested model predictions by experiments with mutant fish such as those

218 exhibiting increased intraocular pressure. Such work exemplifies the power of an
219 approach in which experiments and computational models are tightly integrated.

220

221 *Ft-Ds pathway*

222

223 As discussed above, the *Drosophila* Ft-Ds pathway is required for the planar
224 polarisation of the atypical myosin Dachs. This in turn is required for orienting cell
225 divisions during morphogenesis [37]. More recently a direct correlation between
226 Dachs polarisation, membrane tension and tissue shape during growth has been
227 made using a combination of modelling and mutant clone experiments in the
228 *Drosophila* pupal dorsal thorax [38]. Following from earlier work linking Ft-Ds to
229 mechanical control of morphogenesis [34], the authors explored why Ft or Ds mutant
230 clones are rounded in shape, appearing to minimise their contacts with neighbouring
231 cells, a process which is dependent on Dachs [37]. Notably, Dachs is enriched at
232 clone boundary junctions and reduced at transversal junctions, those perpendicular
233 to the clone boundary within the clone (**Fig. 4C**). This polarisation of Dachs
234 correlated with altered line tension of these junctions. A cellular Potts model, with
235 differences in tension at particular interfaces, was able to accurately recapitulate the
236 clone circularity observed *in vivo*.

237

238 *AP patterning pathway*

239

240 In the *Drosophila* embryo, the aforementioned pair-rule gene expression stripes lead
241 to enrichment of Myosin II at AP borders and the adapter protein Bazooka/Par3 at
242 dorsoventral (DV) borders [45,61], the latter recruiting E-cadherin to form adherens
243 junctions. Planar polarisation of Myosin II, which drives the selective shortening of
244 cell-cell junctions during active cell intercalation in germ-band extension [61], was
245 recently discovered to be mediated by overlapping expression domains of Toll-like
246 receptors [62]. This provides a combinatorial code where every cell along the AP axis
247 has a different 'identity'. To investigate how order is maintained as cells intercalate,
248 Tetley et al [63] combined tissue-scale *in vivo* imaging and analysis with a vertex
249 model incorporating differential junctional line tension between cells of different
250 identities. Boundaries defined by polarised Myosin II, including parasegmental
251 boundaries [47], were found to drive axis extension while at the same time limiting
252 cell mixing. This work highlights the burgeoning recognition of the importance of
253 'cables' and other planar enrichments of actomyosin in coordinating morphogenetic
254 processes. Future modelling efforts should include more mechanically explicit

255 descriptions of how levels and polarisation of Myosin II and other effector proteins
256 modulate cell mechanical properties. A pioneering example of such integration was
257 recently proposed by Lan et al, who coupled modelling of polarisation of Rho-kinase,
258 myosin and Bazooka with a vertex model, but restrict their attention to a relatively
259 small number of cells [64].

260

261

262 **Interplay between mechanics and planar polarity**

263

264 The above work seeks to understand the geometric and mechanical consequences
265 of planar polarity signalling at the tissue level. However, recent evidence points to
266 there being feedback, with adhesion and tension affecting tissue patterning pathways
267 [13]. An extensive study used time-lapse imaging of *Drosophila* pupal wing
268 development over several hours coupled with a vertex model showing that external
269 tension elongates cells along the proximodistal axis and dictates the orientation of
270 planar polarity [65]. Similarly, in the developing *Xenopus* embryo, mechanical strain
271 has been shown to orient the global polarity axis [66]. Furthermore, in the mouse
272 skin, *Celsr1* symmetry appears to be broken by mechanical deformation along one
273 axis [67]. Together, these results suggest a general mechanism where planar polarity
274 proteins perdure on persistent junctions and are slow to accumulate on newly formed
275 junctions allowing oriented cell rearrangements and tissue deformations to induce a
276 new axis of asymmetry [11]. This further suggests that in some contexts core planar
277 polarity polarisation is a passive process, governed by tissue-level changes.

278 Conversely, the *Drosophila* Ft-Ds pathway is able to resist tissue strain and maintain
279 its polarity in response to the graded signal of Fj, suggesting it is actively remodelled
280 [39]. This is an intriguing area for future study where computational modelling may
281 help to unravel why these pathways behave differently.

282

283

284 **Concluding remarks**

285

286 We conclude by highlighting some extensions required to increase the utility of
287 computational models in understanding planar polarity and tissue mechanics during
288 development.

289

290 Several sources of biological complexity have not yet been incorporated or
291 investigated within these models. A key consideration is the timescale over which a

292 tissue can establish or remodel the asymmetric distribution of planar polarity
293 components within a cell, versus the timescale over which mechanical changes
294 occur. Notably, the rate of planar polarisation is likely to be strongly influenced by
295 mechanisms such as directed vesicular transport and recycling of planar polarity
296 components, but these have so far been neglected in current models. Furthermore,
297 the significance of stochasticity and variability in polarity protein interactions and
298 signal interpretation remain to be addressed, even though *in vivo* these are likely to
299 contribute a significant degree of noise.

300

301 While two-dimensional computational models of patterned epithelial have established
302 themselves as important tools, three-dimensional models remain limited and are
303 typically restricted to imposed, static anisotropies in mechanical properties [68]. The
304 extension of such models to allow for the dynamic simulation of planar polarity
305 signalling remains to be tackled. For example, an intriguing link between core
306 pathway planar polarity and three-dimensional tissue deformations was found by
307 Ossipova et al [69], who demonstrated that planar polarity-dependent polarisation of
308 the recycling endosome marker Rab11 is required for apical constriction and
309 subsequent epithelial folding in the *Xenopus* neural plate.

310

311 Several software tools have recently been released for automated cell segmentation,
312 tracking, and shape and polarity quantification in epithelial tissues [70-72]. This has
313 coincided with the development of techniques to measure, infer, and manipulate
314 forces *in vivo* [73,74]. Ongoing technical challenges associated with integrating the
315 resulting data within computational models include developing efficient methods of
316 simulating, and performing parameter inference and uncertainty quantification, on
317 such models. Addressing these challenges will help to place computational models of
318 planar polarity and tissue mechanics on a more quantitative footing, advancing their
319 biological realism and power to guide future experiments.

320

321

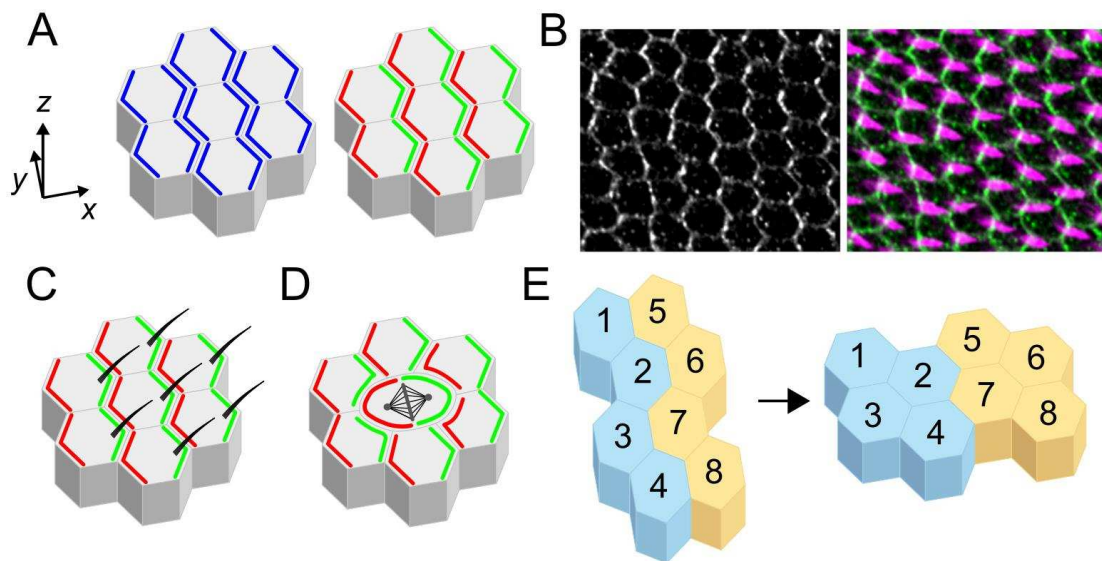
322 **Acknowledgements**

323

324 This work was supported by The Wellcome Trust (grant number 100986) and The
325 University of Sheffield.

326
327

Figure 1

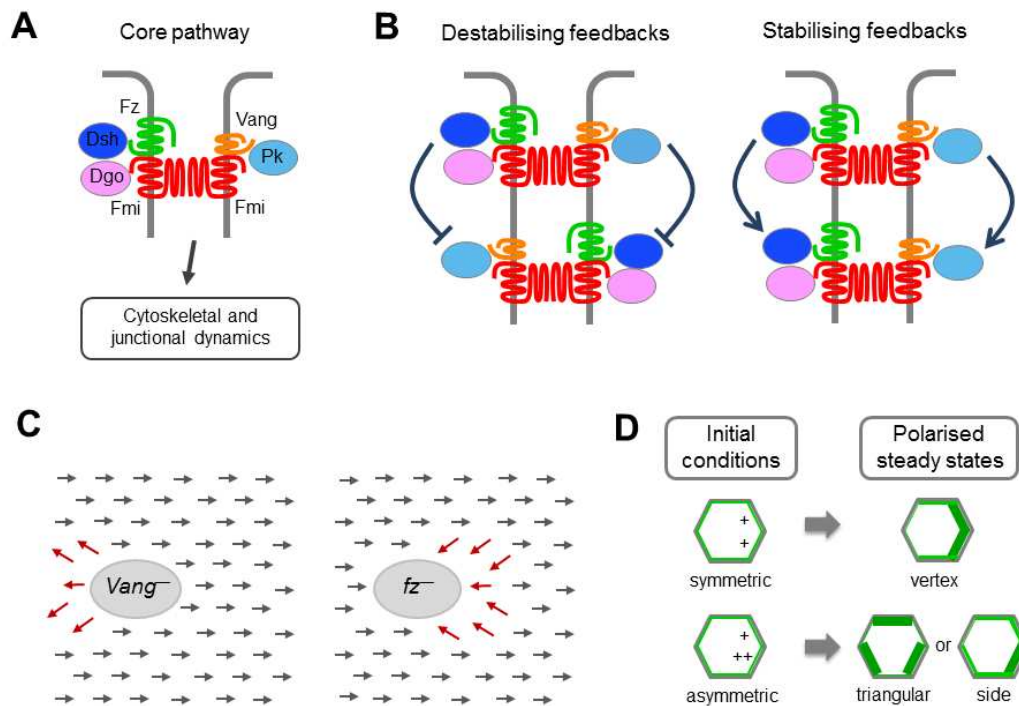


328
329

330 **Planar polarity in epithelial morphogenesis.** (A) In addition to polarising along an
331 apicobasal axis (z), epithelial cells often exhibit planar polarity (also known as planar
332 cell polarity) within the plane of the tissue (x, y). Planar polarity arises from the non-
333 uniform distribution of polarity proteins, which may exhibit axial (enriched on opposite
334 sides of each cell; blue) or vectorial (enriched on one side; red and green) polarity.
335 (B) Wild-type *Drosophila* pupal wing (28h after puparium formation) stained for Vang
336 (grey and green), which has vectorial polarity, and trichomes (magenta) (C, D, E)
337 Planar polarity coordinates the alignment and organisation of cellular and
338 multicellular structures. These include: the formation of hairs and bristles, such as
339 the trichomes produced on the distal side of each cell on the adult *Drosophila* wing
340 surface (C); oriented divisions, as observed for example in cells in *Drosophila*
341 imaginal discs (D); and (E) polarised cell movements and rearrangements, such as
342 during convergent extension.

343
344

Figure 2



345
346

347

Figure 2. Computational modelling of the core pathway in *Drosophila* wing

348

development. (A) Intercellular core protein complex arrangement at the adherens

349

junction zone of *Drosophila* epithelial cells. The formation of an asymmetric

350

intercellular complex involves the transmembrane proteins Frizzled (Fz; green) and

351

Flamingo (Fmi; red) and the cytosolic proteins Dishevelled (Dsh; dark blue) and

352

Diego (Dgo; pink) at the distal end of one cell, and the transmembrane proteins Vang

353

Gogh (Vang; orange) and Fmi and the cytosolic protein Prickle (Pk; pale blue) at the

354

proximal end of the adjacent cell. Polarised localisation of complex components

355

leads to altered cytoskeletal and junctional dynamics, and thus altered cell

356

mechanics. **(B)** Possible feedback interactions between non-transmembrane factors

357

that, either alone or in combinations, could underlie amplification of asymmetry. For

358

example, Dsh may inhibit Pk binding to Vang. **(C)** Schematic of non-autonomous

359

phenotypes, observed in the *Drosophila* wing, around clones of cells mutant for Fz or

360

Vang. **(D)** Schematic of 2D simulation results from Fischer et al [23], showing that the

361

model of Amonlirdviman et al [22] does not give stable vertex polarised steady states

362

in the absence of a persistent global bias. A uniform array of hexagonal cells is

363

considered. In the upper panel, initial conditions are such that Fz is localised in all

364

compartments of each hexagonal cell with a small initial bias (+) in the two distal

365

compartments. This initial bias is amplified by the feedbacks, while symmetry is

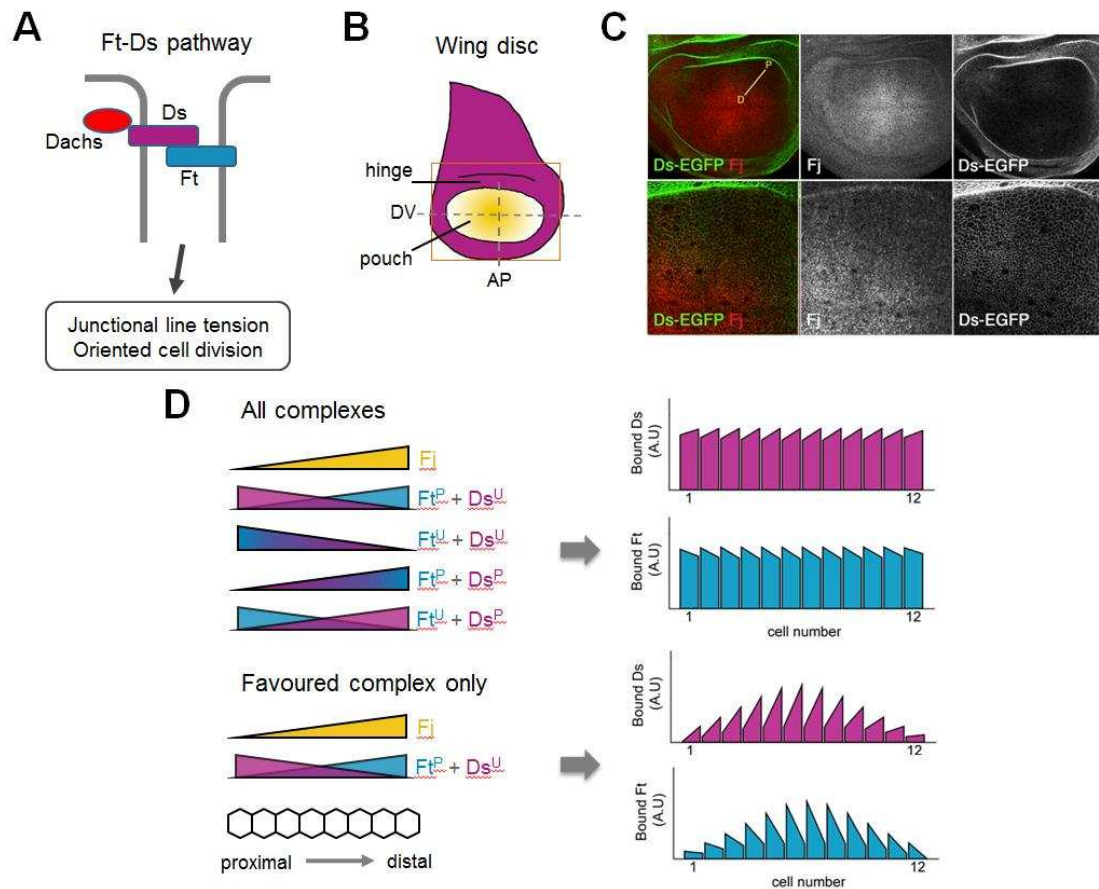
366

maintained, resulting in a final vertex polarity (thicker green edges).

367 panel, an initial bias is applied but with a small difference (either + or ++) between
368 the two distal compartments. Again the initial bias is amplified, but given the noise in
369 initial conditions, vertex polarity is not maintained.

370
371

Figure 3



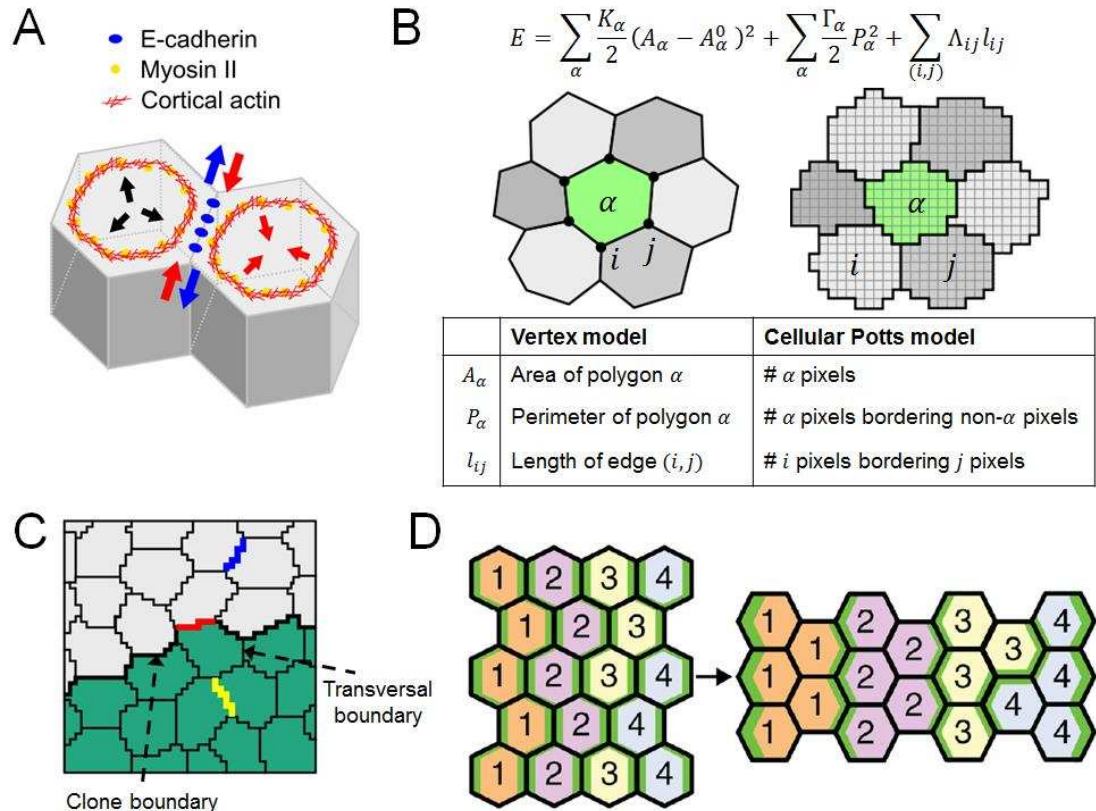
372
373

374 **Figure 3. Computational modelling of Ft-Ds pathway establishment in the**
 375 ***Drosophila* wing.** (A) Fat (Ft; turquoise) and Dachsous (Ds; purple) bind
 376 heterophilically to form asymmetric intercellular complexes. Dachs (red), an atypical
 377 myosin, is recruited to colocalise with Ds, where it modulates junctional tension and
 378 orients cell division. (B) Cartoon of *Drosophila* 3rd instar larval wing disc. Ds (purple)
 379 is expressed at high levels in the hinge region, whereas Four-jointed (Fj; yellow) is
 380 expressed in a graded pattern in the pouch, which will go on to form the blade of the
 381 adult wing. Dorsoventral (DV) and anterioposterior (AP) compartment boundaries are
 382 shown by dashed lines. Orange box represents the cropped region shown in the
 383 upper panels of C. (C) Anti-Fj staining (red) of a wing disc expressing Ds-EGFP
 384 (green) as shown in Hale et al [42]. Fj is clearly graded along the proximodistal (PD)
 385 axis. (D) Simulation results based on the computational model of Hale et al [42].
 386 Graded Fj leads to opposing gradients of phosphorylated Ft/Ds (Ft^P, Ds^P) and
 387 unphosphorylated Ft/Ds (Ft^U, Ds^U). Upper panel - all four possible heterophilic
 388 complexes form, listed in order of preferential binding (i.e. the top complex is the
 389 most favoured), leading to cellular asymmetry of bound Ft and Ds complexes that are
 390 largely uniform across the tissue. Lower panel - only the most favoured complex

391 forms (Ft^P binding Ds^U), thus polarisation and bound protein levels are much stronger
392 in the middle of the tissue compared to the proximal and distal edges. Graphs show
393 simulation results where each bar represents a cell, showing the relative amount of
394 bound protein on the left and right sides in arbitrary units (A.U.).

395
396

Figure 4



397
398
399

Figure 4. Computational modelling of the mechanics of planar polarised

400

epithelia. (A) Schematic of the forces arising from apically localised adhesion

401

molecules and cytoskeletal components in neighbouring epithelial cells. E-cadherin

402

binding between tends to reduce surface tension and expand cell-cell junctions (blue

403

arrows), while actomyosin imposes contractile forces at junctions and cell cortices

404

(red arrows), the latter counteracted by intracellular osmotic pressure (black arrows).

405

Each of these effector proteins can be regulated by upstream planar polarity signals.

406

(B) Comparison of the vertex and cellular Potts models of epithelial dynamics. Either

407

a force balance equation for each vertex (left) or Monte Carlo simulation and

408

exchange of pixels (right) is used to drive the tissue toward a configuration of

409

minimum 'energy', E . **(C)** Cellular Potts model of somatic clone rounding in

410

Drosophila pupal dorsal thorax [34]. Observed cell behaviours in Ft or Ds mutant

411

clones are recapitulated by assuming that Dachs polarisation results in line tensions

412

(Λ_{ij}) taking a high value for cell-cell junctions at a clone boundary (red), an

413

intermediate value for cell-cell junctions outside the clone (blue), and a low value for

414

cell-cell junctions within the clone (yellow). **(D)** Vertex model of active cell

415

intercalation during *Drosophila* germ-band extension [63]. Cell rearrangement results

416

in stripes of cells of the same identity becoming adjacent. Myosin II is enriched

417 preferentially at interfaces shared between cells of different identity (green).
418 Convergent extension can be recapitulated by assuming that line tensions at cell-cell
419 junctions (Λ_{ij}) are increased by Myosin II enrichment and depend nonlinearly on the
420 total length of contiguous interfaces a given cell has with cells of different identities,
421 the latter assumption approximating the presence of actomyosin cables.

422 **Reference annotations**

423

424 **Bosveld F et al. Development 2016, 143:623-634.**

425 (••) This elegant study combines experiments in *Drosophila* pupal dorsal thorax with
426 a cellular Potts model to analyse why Ft or Ds mutant clones are rounded in shape.
427 The authors find that Dachs polarisation correlates with changes in junctional tension
428 within a clone and at its boundary. This work highlights the connection between
429 Dachs localisation, polarised membrane tension and tissue shape during growth.

430

431 **Hale et al. Elife 2015, 4.**

432 (•) In this study, a 1D ODE model is used to assess different scenarios for how a Fj
433 gradient could influence planar polarisation of Ft and Ds in the *Drosophila* wing, with
434 predictions tested *in vivo*. This work demonstrates for the first time that Fj acts on
435 both Ft and Ds *in vivo*, and is sufficient to explain the observed pattern of Ft–Ds
436 binding and planar polarisation across the wing.

437

438 **Tetley et al. Elife 2016, 5.**

439 (••) This study combines detailed quantitative data analysis with computational
440 modelling to elucidate how Myosin II planar polarisation drives active cell
441 rearrangements during *Drosophila* germ-band extension. To account for the
442 observed tissue-scale behaviours, the authors develop the first vertex model that can
443 account for differential contractility on either side of a cell-cell interface, allowing for
444 junctional sliding.

445

446 **Lan et al. Phys Biol. 12, 56011**

447 (••) This computational study couples a model of polarisation of Rho-kinase, myosin
448 and Bazooka with a vertex model to understand the interplay between planar polarity
449 and coordinated cell movement and shape changes in *Drosophila* germ-band
450 extension. The authors present one of the first cell-based models of epithelial
451 mechanics that integrates a kinetic description of intracellular signalling and
452 polarisation and their effect on cell mechanics.

453

454 **Chien et al. Curr Biol 2015, 25:2774-2784.**

455 (•) This experimental study shows for the first time that during *Xenopus* gastrulation,
456 mechanical strain on apical microtubules is both necessary and sufficient to direct a
457 global axis of planar polarity.

458

459 **Aw et al. Curr Biol 2016, 26:2090-2100.**

460 (•) This experimental study demonstrates that planar polarity axis development in the
461 mouse epidermis correlates with tissue-scale deformations that induce cell
462 rearrangements. Furthermore, Celsr1 asymmetry is induced by remodelling of cell
463 junctions.

464

465 **Farrell et al. Development 2017, 144:1725-1734.**

466 (•) This work exemplifies recent efforts by the community to develop robust
467 computational tools for quantifying cell shape, movement and polarity in epithelial
468 tissues. The authors demonstrate the utility of their open-source software by
469 analysing cell polarity during *Drosophila* germ-band extension.

470

471 **References**

472

- 473 1. Green JB, Sharpe J: **Positional information and reaction-diffusion: two big**
474 **ideas in developmental biology combine.** *Development* 2015, **142**:1203-1211.
- 475 2. LeGoff L, Lecuit T: **Mechanical Forces and Growth in Animal Tissues.** *Cold*
476 *Spring Harb Perspect Biol* 2015, **8**:a019232.
- 477 3. Eder D, Aegerter C, Basler K: **Forces controlling organ growth and size.** *Mech*
478 *Dev* 2017, **144**:53-61.
- 479 4. Julicher F, Eaton S: **Emergence of tissue shape changes from collective cell**
480 **behaviours.** *Semin Cell Dev Biol* 2017.
- 481 5. Thompson BJ: **Cell polarity: models and mechanisms from yeast, worms and**
482 **flies.** *Development* 2013, **140**:13-21.
- 483 6. Goodrich LV, Strutt D: **Principles of planar polarity in animal development.**
484 *Development* 2011, **138**:1877-1892.
- 485 7. Hale R, Strutt D: **Conservation of Planar Polarity Pathway Function Across**
486 **the Animal Kingdom.** *Annu Rev Genet* 2015, **49**:529-551.
- 487 8. Burak Y, Shraiman BI: **Order and stochastic dynamics in Drosophila planar**
488 **cell polarity.** *PLoS Comput Biol* 2009, **5**:e1000628.
- 489 9. Ma D, Yang CH, McNeill H, Simon MA, Axelrod JD: **Fidelity in planar cell**
490 **polarity signalling.** *Nature* 2003, **421**:543-547.
- 491 10. Butler MT, Wallingford JB: **Planar cell polarity in development and disease.**
492 *Nat Rev Mol Cell Biol* 2017.
- 493 11. Aw WY, Devenport D: **Planar cell polarity: global inputs establishing cellular**
494 **asymmetry.** *Curr Opin Cell Biol* 2017, **44**:110-116.
- 495 12. Bayly R, Axelrod JD: **Pointing in the right direction: new developments in the**
496 **field of planar cell polarity.** *Nat Rev Genet* 2011, **12**:385-391.
- 497 13. Heller E, Fuchs E: **Tissue patterning and cellular mechanics.** *J Cell Biol* 2015,
498 **211**:219-231.
- 499 14. Morelli LG, Uriu K, Ares S, Oates AC: **Computational approaches to**
500 **developmental patterning.** *Science* 2012, **336**:187-191.
- 501 15. Strutt H, Strutt D: **Asymmetric localisation of planar polarity proteins:**
502 **Mechanisms and consequences.** *Semin Cell Dev Biol* 2009, **20**:957-963.
- 503 16. Vinson CR, Adler PN: **Directional non-cell autonomy and the transmission of**
504 **polarity information by the frizzled gene of Drosophila.** *Nature* 1987,
505 **329**:549-551.
- 506 17. Taylor J, Abramova N, Charlton J, Adler PN: **Van Gogh: a new Drosophila**
507 **tissue polarity gene.** *Genetics* 1998, **150**:199-210.

- 508 18. Strutt D, Strutt H: **Differential activities of the core planar polarity proteins**
509 **during Drosophila wing patterning.** *Dev Biol* 2007, **302**:181-194.
- 510 19. Tree DR, Shulman JM, Rousset R, Scott MP, Gubb D, Axelrod JD: **Prickle**
511 **mediates feedback amplification to generate asymmetric planar cell**
512 **polarity signaling.** *Cell* 2002, **109**:371-381.
- 513 20. Jenny A, Reynolds-Kenneally J, Das G, Burnett M, Mlodzik M: **Diego and**
514 **Prickle regulate Frizzled planar cell polarity signalling by competing for**
515 **Dishevelled binding.** *Nat Cell Biol* 2005, **7**:691-697.
- 516 21. Axelrod JD, Tomlin CJ: **Modeling the control of planar cell polarity.** *Wiley*
517 *Interdiscip Rev Syst Biol Med* 2011, **3**:588-605.
- 518 22. Amonlirdviman K, Khare NA, Tree DR, Chen WS, Axelrod JD, Tomlin CJ:
519 **Mathematical modeling of planar cell polarity to understand domineering**
520 **nonautonomy.** *Science* 2005, **307**:423-426.
- 521 23. Fischer S, Houston P, Monk NA, Owen MR: **Is a persistent global bias**
522 **necessary for the establishment of planar cell polarity?** *PLoS One* 2013,
523 **8**:e60064.
- 524 24. Le Garrec JF, Lopez P, Kerszberg M: **Establishment and maintenance of**
525 **planar epithelial cell polarity by asymmetric cadherin bridges: a computer**
526 **model.** *Dev Dyn* 2006, **235**:235-246.
- 527 25. Hazelwood LD, Hancock JM: **Functional modelling of planar cell polarity: an**
528 **approach for identifying molecular function.** *BMC Dev Biol* 2013, **13**:20.
- 529 26. Abley K, De Reuille PB, Strutt D, Bangham A, Prusinkiewicz P, Maree AF,
530 Grieneisen VA, Coen E: **An intracellular partitioning-based framework for**
531 **tissue cell polarity in plants and animals.** *Development* 2013, **140**:2061-2074.
- 532 27. Schamberg S, Houston P, Monk NA, Owen MR: **Modelling and analysis of**
533 **planar cell polarity.** *Bull Math Biol* 2010, **72**:645-680.
- 534 28. Ma D, Amonlirdviman K, Raffard RL, Abate A, Tomlin CJ, Axelrod JD: **Cell**
535 **packing influences planar cell polarity signaling.** *Proc Natl Acad Sci U S A*
536 2008, **105**:18800-18805.
- 537 29. Shimada Y, Yonemura S, Ohkura H, Strutt D, Uemura T: **Polarized transport of**
538 **Frizzled along the planar microtubule arrays in Drosophila wing epithelium.**
539 *Dev Cell* 2006, **10**:209-222.
- 540 30. Matis M, Russler-Germain DA, Hu Q, Tomlin CJ, Axelrod JD: **Microtubules**
541 **provide directional information for core PCP function.** *Elife* 2014, **3**:e02893.
- 542 31. Thomas C, Strutt D: **The roles of the cadherins Fat and Dachsous in planar**
543 **polarity specification in Drosophila.** *Dev Dyn* 2012, **241**:27-39.

- 544 32. Simon MA, Xu A, Ishikawa HO, Irvine KD: **Modulation of fat:dachsous binding**
545 **by the cadherin domain kinase four-jointed.** *Curr Biol* 2010, **20**:811-817.
- 546 33. Brittle AL, Repiso A, Casal J, Lawrence PA, Strutt D: **Four-jointed modulates**
547 **growth and planar polarity by reducing the affinity of dachsous for fat.** *Curr*
548 *Biol* 2010, **20**:803-810.
- 549 34. Bosveld F, Bonnet I, Guirao B, Tlili S, Wang Z, Petitalot A, Marchand R, Bardet
550 PL, Marcq P, Graner F, et al.: **Mechanical control of morphogenesis by**
551 **Fat/Dachsous/Four-jointed planar cell polarity pathway.** *Science* 2012,
552 **336**:724-727.
- 553 35. Ambegaonkar AA, Pan G, Mani M, Feng Y, Irvine KD: **Propagation of**
554 **Dachsous-Fat planar cell polarity.** *Curr Biol* 2012, **22**:1302-1308.
- 555 36. Willecke M, Hamaratoglu F, Sansores-Garcia L, Tao C, Halder G: **Boundaries of**
556 **Dachsous Cadherin activity modulate the Hippo signaling pathway to**
557 **induce cell proliferation.** *Proc Natl Acad Sci U S A* 2008, **105**:14897-14902.
- 558 37. Mao Y, Tournier AL, Bates PA, Gale JE, Tapon N, Thompson BJ: **Planar**
559 **polarization of the atypical myosin Dachs orientes cell divisions in**
560 **Drosophila.** *Genes Dev* 2011, **25**:131-136.
- 561 38. Bosveld F, Guirao B, Wang Z, Riviere M, Bonnet I, Graner F, Bellaiche Y:
562 **Modulation of junction tension by tumor suppressors and proto-oncogenes**
563 **regulates cell-cell contacts.** *Development* 2016, **143**:623-634.
- 564 39. Merkel M, Sagner A, Gruber FS, Etournay R, Blasse C, Myers E, Eaton S,
565 Julicher F: **The balance of prickle/spiny-legs isoforms controls the amount**
566 **of coupling between core and fat PCP systems.** *Curr Biol* 2014, **24**:2111-
567 2123.
- 568 40. Mani M, Goyal S, Irvine KD, Shraiman BI: **Collective polarization model for**
569 **gradient sensing via Dachsous-Fat intercellular signaling.** *Proc Natl Acad*
570 *Sci U S A* 2013, **110**:20420-20425.
- 571 41. Jolly MK, Rizvi MS, Kumar A, Sinha P: **Mathematical modeling of sub-cellular**
572 **asymmetry of fat-dachsous heterodimer for generation of planar cell**
573 **polarity.** *PLoS One* 2014, **9**:e97641.
- 574 42. Hale R, Brittle AL, Fisher KH, Monk NA, Strutt D: **Cellular interpretation of the**
575 **long-range gradient of Four-jointed activity in the Drosophila wing.** *Elife*
576 2015, **4**.
- 577 43. Irvine KD, Wieschaus E: **Cell intercalation during Drosophila germband**
578 **extension and its regulation by pair-rule segmentation genes.** *Development*
579 1994, **120**:827-841.

- 580 44. Blankenship JT, Backovic ST, Sanny JS, Weitz O, Zallen JA: **Multicellular**
581 **rosette formation links planar cell polarity to tissue morphogenesis.** *Dev*
582 *Cell* 2006, **11**:459-470.
- 583 45. Zallen JA, Wieschaus E: **Patterned gene expression directs bipolar planar**
584 **polarity in *Drosophila*.** *Dev Cell* 2004, **6**:343-355.
- 585 46. da Silva SM, Vincent JP: **Oriented cell divisions in the extending germband**
586 **of *Drosophila*.** *Development* 2007, **134**:3049-3054.
- 587 47. Butler LC, Blanchard GB, Kabla AJ, Lawrence NJ, Welchman DP, Mahadevan L,
588 Adams RJ, Sanson B: **Cell shape changes indicate a role for extrinsic tensile**
589 **forces in *Drosophila* germ-band extension.** *Nat Cell Biol* 2009, **11**:859-864.
- 590 48. Akam M: **The molecular basis for metameric pattern in the *Drosophila***
591 **embryo.** *Development* 1987, **101**:1-22.
- 592 49. Jaeger J, Surkova S, Blagov M, Janssens H, Kosman D, Kozlov KN, Manu,
593 Myasnikova E, Vanario-Alonso CE, Samsonova M, et al.: **Dynamic control of**
594 **positional information in the early *Drosophila* embryo.** *Nature* 2004,
595 **430**:368-371.
- 596 50. Verd B, Crombach A, Jaeger J: **Dynamic Maternal Gradients Control Timing**
597 **and Shift-Rates for *Drosophila* Gap Gene Expression.** *PLoS Comput Biol*
598 2017, **13**:e1005285.
- 599 51. Guillot C, Lecuit T: **Mechanics of epithelial tissue homeostasis and**
600 **morphogenesis.** *Science* 2013, **340**:1185-1189.
- 601 52. Wallingford JB: **Planar cell polarity and the developmental control of cell**
602 **behavior in vertebrate embryos.** *Annu Rev Cell Dev Biol* 2012, **28**:627-653.
- 603 53. Devenport D: **The cell biology of planar cell polarity.** *J Cell Biol* 2014,
604 **207**:171-179.
- 605 54. Warrington SJ, Strutt H, Strutt D: **The Frizzled-dependent planar polarity**
606 **pathway locally promotes E-cadherin turnover via recruitment of RhoGEF2.**
607 *Development* 2013, **140**:1045-1054.
- 608 55. Classen AK, Anderson KI, Marois E, Eaton S: **Hexagonal packing of**
609 ***Drosophila* wing epithelial cells by the planar cell polarity pathway.** *Dev Cell*
610 2005, **9**:805-817.
- 611 56. Fletcher AG, Cooper F, Baker RE: **Mechanocellular models of epithelial**
612 **morphogenesis.** *Philos Trans R Soc Lond B Biol Sci* 2017, **372**.
- 613 57. Fletcher AG, Osterfield M, Baker RE, Shvartsman SY: **Vertex models of**
614 **epithelial morphogenesis.** *Biophys J* 2014, **106**:2291-2304.

- 615 58. Marée AF, Grieneisen VA, Hogeweg P: **The Cellular Potts Model and**
616 **biophysical properties of cells, tissues and morphogenesis.** In *Single-cell-*
617 *based models in biology and medicine.* Edited by: Springer; 2007:107-136.
- 618 59. Osborne JM, Fletcher AG, Pitt-Francis JM, Maini PK, Gavaghan DJ: **Comparing**
619 **individual-based approaches to modelling the self-organization of**
620 **multicellular tissues.** *PLoS Comput Biol* 2017, **13**:e1005387.
- 621 60. Salbreux G, Barthel LK, Raymond PA, Lubensky DK: **Coupling mechanical**
622 **deformations and planar cell polarity to create regular patterns in the**
623 **zebrafish retina.** *PLoS Comput Biol* 2012, **8**:e1002618.
- 624 61. Bertet C, Sulak L, Lecuit T: **Myosin-dependent junction remodelling controls**
625 **planar cell intercalation and axis elongation.** *Nature* 2004, **429**:667-671.
- 626 62. Pare AC, Vichas A, Fincher CT, Mirman Z, Farrell DL, Mainieri A, Zallen JA: **A**
627 **positional Toll receptor code directs convergent extension in Drosophila.**
628 *Nature* 2014, **515**:523-527.
- 629 63. Tetley RJ, Blanchard GB, Fletcher AG, Adams RJ, Sanson B: **Unipolar**
630 **distributions of junctional Myosin II identify cell stripe boundaries that**
631 **drive cell intercalation throughout Drosophila axis extension.** *Elife* 2016, **5**.
- 632 64. Lan H, Wang Q, Fernandez-Gonzalez R, Feng JJ: **A biomechanical model for**
633 **cell polarization and intercalation during Drosophila germband extension.**
634 *Phys Biol* 2015, **12**:056011.
- 635 65. Aigouy B, Farhadifar R, Staple DB, Sagner A, Roper JC, Julicher F, Eaton S:
636 **Cell flow reorients the axis of planar polarity in the wing epithelium of**
637 **Drosophila.** *Cell* 2010, **142**:773-786.
- 638 66. Chien YH, Keller R, Kintner C, Shook DR: **Mechanical strain determines the**
639 **axis of planar polarity in ciliated epithelia.** *Curr Biol* 2015, **25**:2774-2784.
- 640 67. Aw WY, Heck BW, Joyce B, Devenport D: **Transient Tissue-Scale Deformation**
641 **Coordinates Alignment of Planar Cell Polarity Junctions in the Mammalian**
642 **Skin.** *Curr Biol* 2016, **26**:2090-2100.
- 643 68. Bielmeier C, Alt S, Weichselberger V, La Fortezza M, Harz H, Julicher F,
644 Salbreux G, Classen AK: **Interface Contractility between Differently Fated**
645 **Cells Drives Cell Elimination and Cyst Formation.** *Curr Biol* 2016, **26**:563-
646 574.
- 647 69. Ossipova O, Kim K, Lake BB, Itoh K, Ioannou A, Sokol SY: **Role of Rab11 in**
648 **planar cell polarity and apical constriction during vertebrate neural tube**
649 **closure.** *Nat Commun* 2014, **5**:3734.

- 650 70. Heller D, Hoppe A, Restrepo S, Gatti L, Tournier AL, Tapon N, Basler K, Mao Y:
651 **EpiTools: An Open-Source Image Analysis Toolkit for Quantifying**
652 **Epithelial Growth Dynamics.** *Dev Cell* 2016, **36**:103-116.
- 653 71. Farrell DL, Weitz O, Magnasco MO, Zallen JA: **SEGGA: a toolset for rapid**
654 **automated analysis of epithelial cell polarity and dynamics.** *Development*
655 2017, **144**:1725-1734.
- 656 72. Etournay R, Merkel M, Popovic M, Brandl H, Dye NA, Aigouy B, Salbreux G,
657 Eaton S, Julicher F: **TissueMiner: A multiscale analysis toolkit to quantify**
658 **how cellular processes create tissue dynamics.** *Elife* 2016, **5**.
- 659 73. Sugimura K, Lenne PF, Graner F: **Measuring forces and stresses in situ in**
660 **living tissues.** *Development* 2016, **143**:186-196.
- 661 74. Bambardekar K, Clement R, Blanc O, Chardes C, Lenne PF: **Direct laser**
662 **manipulation reveals the mechanics of cell contacts in vivo.** *Proc Natl Acad*
663 *Sci U S A* 2015, **112**:1416-1421.